Pollution, 5(4): 775-788, Autumn 2019
DOI: 10.22059/poll.2019.273769.565
Print ISSN: 2383-451X Online ISSN: 2383-4501
Web Page: https://jpoll.ut.ac.ir, Email: jpoll@ut.ac.ir

The Use of Raw and Thermally-Modified Calcareous Sludge Generated in Stone Cutting Industry for Sulfur Dioxide Removal

Loghmani, F., Mirghaffari, N* and Soleimani, M.

Department of Natural Resources, Isfahan University of Technology, 84156-83111, Isfahan, Iran

Received: 13.01.2019 Accepted: 05.06.2019

ABSTRACT: Management of solid wastes is considered as an economic and environmental issue in the building stone industry. The current study uses raw and calcined calcareous sludge, generated in the stone cutting factories, in order to remove sulfur dioxide. Sludge characterization has been performed, using X-ray fluorescence (XRF), X-ray diffraction (XRD), scanning electron microscopy (SEM), and energy-dispersive X-ray spectroscopy (EDX) analyses. The removal experiments of sulfur dioxide have conducted under different humid contents and adsorbent doses. The results showed that the higher the adsorbent dosage and humidity content, the greater the SO2 adsorption.. The calcination process at temperatures of 400, 500, 600, and 700℃ revealed that with rising calcination temperature and humidity content, the adsorbent capability is enhanced considerably. This method could be developed for the management of stone sludge produced from the stone cutting industry through its conversion into an effective and low-cost adsorbent for desulfurization process.

Keywords: Adsorbent, Adsorption, Calcination, Air pollution.

INTRODUCTION

A great part of the electrical energy, generated in the world, is supplied by power plants, which use fossil fuels emitting different pollutants and greenhouse gases to the atmosphere (Yang et al., 2008). Sulfur dioxide (SO_2) is one of the most important pollutant gasses. A highly reactive gas, it is generated from fossil fuel combustion like coal and oil in power plants. Acid rain, human and animal respiration illnesses, and harmful effects on vegetation are the most important environmental impacts of SO_2 (Chakrabarti, 2001). In this regard, the necessity of SO_2 emission control by effective methods has been the subject of intense interest. Nowadays, scientists propose a wide variety of approaches to control sulfur dioxide emission, such as sulfur dioxide removal in the feed and the use of technologies such as fuel gas desulfurization (FGD) (Nath & Stefanov Cholakov, 2009). FGD is defined as the process of sulfur dioxide elimination from fuel gases generally by calcareous adsorbents such as lime and limestone. FGD processes are classified into different types. For example, it is divided into regenerable and non-regenerable methods depending on the possibility of sulfur separation from the adsorbents. Moreover, it could be a wet or dry process based on the presence of water in the adsorbent or even in the flue gas (Córdoba, 2015). In fact, during FGD process, sulfur dioxide as an acidic gas is removed through reaction with alkali materials (Rayaprolu, 2017).

* Corresponding Author, Email: mnorolah@cc.iut.ac.ir

The most common adsorbents widely used in the industrial flue gas desulfurization units are calcareous compounds including limestone ($CaCO_3$), lime (CaO), and hydrated lime ($Ca(OH)_2$) (Suárez-Ruiz & Crelling, 2008). The calcareous adsorbents, which are very efficient in removal of sulfur dioxide, are used in numerous coal power plants (Miao et al., 2015). Calcium carbonate is an abundant and cheap substance that can be simply converted to calcium oxide and calcium hydroxide. Generally, the calcium-based rocks could be appropriate for use in FGD processes due to the presence of different metal oxides. Xie et al. (2010) reported that complex metal oxides are much more effective for desulfurization processes than single metal oxides (Xie et al., 2010). The natural stones derived from earth's crust are one of the important building materials, considered as a source of metal oxides (Lees & Payne, 2001). These stones are a mixture of two or more minerals mainly strong, durable, and descent in appearance (Gopi, 2009). After extracting the stones in the mines, they are transferred to stone cutting units in order to have them reformed, reshaped, and converted to usable forms.

The most active stone producing countries in 2012 were China, Turkey, India, Iran, and Italy with about 72% of stone production in the globe. Iran produces about 16.1 million tons of decorative stones from 1203 active quarries, in which Travertine and Marble are estimated to account for some 6.55 and 4.85 tons, respectively, while the remaining 4.69 tons belongs to other types of stones, like Chrystal Marble, Onyx, and Granite (Lorpari Zanganeh & Roosta, 2012).

The building stone industry generates a huge amount of solid wastes during its different processes like block squaring, cutting into slab and strip, polishing, and chamfering (Lakhani et al., 2014). Generally, these wastes are classified into two groups, including the fragments with diverse dimensions and stone slurry due to physical processes like extraction, sawing, and polishing (Almeida et al., 2007). The disposal of solid wastes is considered an economic and environmental problem in building stone industry. Several studies, concerning the application of stone wastes, have shown that they can be used for the production of self-compact concrete (SCC), artificial stones, floor tiles, mortars, bricks, PVC pipes, blocks, pottery, filler, binder, and additives to develop alternative building materials and soil stabilization (Al-Joulani, 2007; Al-Joulani, 2014; Alzboon & Mahasneh, 2009; Barani & Esmaili, 2016; Khalilzadeh Shirazi, 2007; Pappu et al., 2007). The possibility of using calcareous stone wastes as an adsorbent for SO_2 removal in the FGD process has been reported in the literature (Altun, 2014; Maina & Mbarawa, 2012; Ogenga et al., 2010; Siagi et al., 2007). In this regard, the blend of lime and other wastes such as iron scraps have also been employed (Maina & Mbarawa, 2012). Previous studies, concerning SO_2 removal by calcareous stone wastes have mainly involved the use of broken rocks, while stone sludge, being in the form of fine powders and abundantly produced in the precipitation ponds, pose more environmental problems for stone cutting industry. These wastes are usually dumped in selected sites with a significant transportation fee; therefore, their utilization as adsorbent for removal of pollutant gases could be important from environmental and economic aspects.

The present study uses raw and thermally-modified sorbent for the adsorption of sulfur dioxide. It also investigates the effect of some parameters such as calcination temperature and adsorbent humidity content on efficiency of prepared adsorbent for SO_2 adsorption.

MATERIALS AND METHODS

Stone sludge was provided from a stone

industry town of Isfahan province, Iran. It was generated during the deposition of marble and travertine particles in sedimentation ponds. The samples were dried at 110℃ for 16 hours, then to get crushed and sieved to a particle size of 106-250 µm.

X-ray Fluorescence (XRF) was used to determine the samples' elemental concentration by weight (S4 PIONEER) with X-ray diffraction (XRD, Philips X'pert PRO) analysis, carried out to identify the chemical composition, the crystal structure, and the particle size of adsorbents (Saravanan & Rani, 2011). This apparatus was equipped with variable divergence and receiving slits with Cu-Ka radiation. The diffraction angle (2Ɵ) of 10- 80° was used for the raw sample and 0-130° for the calcined adsorbant. The shape and size of adsorbent particles were determined, using scanning electron microscopy (SEM, EF-SEM HITACHI) with an accuracy of ±5 nm coupled with the EDX analysis apparatus device (Seron AIS 2300) (Sahoo et al., 2011). The surface area and pore volume analysis of uncalcined and calcined samples were conducted via Brunauer-Emmett-Teller (BET) method. Based on the features of adsorbed gas and pressure (Gladysz & Chawla, 2014) in general, the method employed surface adsorption of N_2 here (with 99.99% purity) at 77K. Sample's surface area and microspore area were computed by means of BET equation. The BJH (Barret, Joyner, and Halenda) method was applied to determine pore size distribution from nitrogen desorption data with an accuracy of ±0.001 m^2/g for surface area and ±0.35-200 nm for pore diameter.

The ability of stone sludge powder for adsorption of SO_2 was studied using a laboratory-scale fixed bed (Fig. 1). The reaction zone was placed in a stainless-steel tube, 30 cm long and 1 cm in inner diameter. Different amounts of adsorbents were utilized to survey the effect of adsorbent dosage, followed by testing the impact of adsorbent humidity content and calcination temperature. The adsorbents were packed in the central part of the reactor and supported by a 100 µm stainless steel mesh. The desulfurization experiments were performed at 1 Pa pressure and 25℃. The gas composition (Vol. %) was 0.5 SO_2 (588 ppm) and 0.5 N_2. Carbon dioxide and oxygen were not used in the experiments as they can affect SO_2 uptake of the adsorbent at low temperatures (Lin et al., 2003). The total flow rate of mixed gases was adjusted to 50 ml/min with a flow meter (HITACHI, AERA FC-7800 CD) apparatus. All experiments were done for 25 minutes, during which time the concentration of outlet gas was constantly monitored by an MRU Vario Plus gas analyzer at 1-min intervals. Prior to the desulfurization tests, the blank run was tested without the presence of adsorbent and humidity, with humidification process enacted through addition of 0.1, 0.05, and 0.01 ml distill water to 1 g of adsorbent.

Each experiment was performed in triplicate. The adsorption percentage was calculated by Eq. (1) and the average of the results was taken.

$$\%SO_2\ Removal\ Efficiency = \frac{C_t - C_0}{C_0} \times 100$$

where C_0 and C_t are sulfur dioxide concentration in the inlet and outlet at time t, respectively.

To investigate the effect of calcination temperature on adsorbent efficiency, the samples were calcined at temperatures of 400, 500, 600, and 700°C in an electric furnace for 1 h. The calcination reaction was endothermic, which means that the forward reaction was favored by higher temperatures (Stanmore & Gilot, 2005).

$$CaCO_3 \rightarrow CaO + CO_2 \quad \Delta H = +182.1\ kJ / mol$$

After calcination, all samples were kept in a closed experimental bottle to avoid any reaction with carbon dioxide (CO_2) and humidity in the air prior to use.

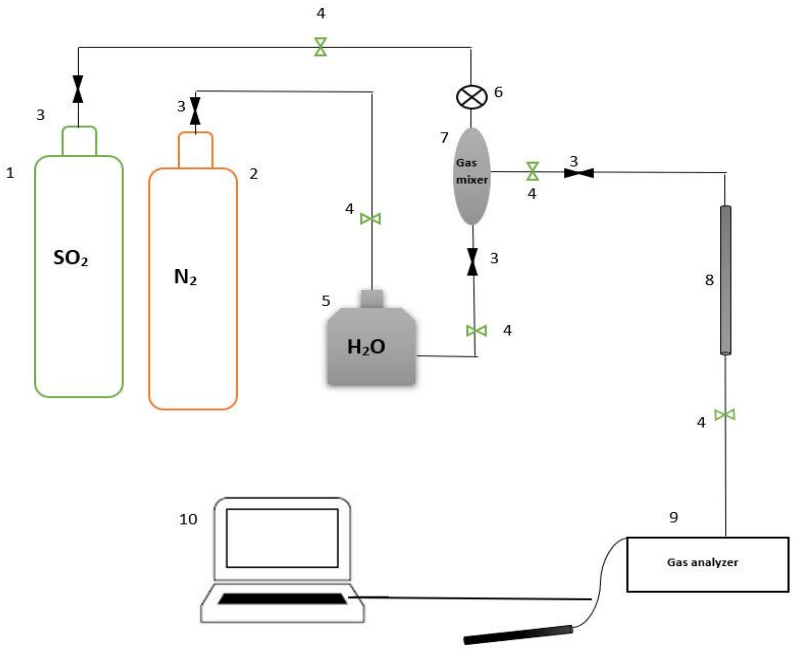

Fig. 1. The schematic design of experimental apparatuses (1: SO_2 cylinder, 2: N_2 cyliner, 3: mass flow controller, 4: valve, 5: water bath, 6: barometer, 7: gas blender, 8: reactor, 9: gas analyzer, and 10: computer)

RESULTS AND DISCUSSION

Table 1 gives the results from XRF analysis of the stone sludge powder. According to XRF analysis, CaO was the most plentiful compound in the stone sludge powder with 44.2 w/w%. Hamisah et al. (2016) studied the characteristics of β-wollastonite, derived from rice straw ash and limestone (Ismail et al., 2016), whose XRF analysis of the limestone also showed that CaO was the most abundant compound. What is more, other compounds, e.g., MgO, Al_2O_3, Si_2O, and Fe_2O_3 were also detected in the stone sludge powder in the present study.

Table 1. XRF analysis of stone sludge powder

Compounds	%(W/W)
CaO	44.22
Fe_2O_3	2.37
Si_2O	1.44
MgO	0.418
ZnO	0.398
Others	0.60
LOI*	50.4

*Loss of ignition

Results from XRD analysis of uncalcined show that $CaCO_3$ was the main component of stone sludge powder and the carbonate calcium phase was predominant. Fig. 2 represents the peaks of stone sludge powder in angles (2Θ) including 23.5°, 29.8°, 31.9°, 36.5°, 39.8°, 43.5°, 47.9°, 48.9°, 57.8°, 61.2°, 63.5°, 65.1°, 66.0°, 70.7°, 73.3°, and 77.6°, which are the peaks of calcite ($CaCO_3$). This analysis also shows that the crystal structure of uncalcined stone sludge powder was Rhombohedral, the morphology of which is characteristic of calcite and dolomite crystals (Souza & Braganca, 2017).

XRD analysis was also carried out on the sorbent, calcined at 700℃ as an optimized variety. According to the results from this analysis during the calcination, calcium carbonate was decomposed and CaO was partially formed (Fig. 3). Based on Fig. 2b, some peaks of CaO appeared at 2θ of 32.2°, 37.3°, and 53.8°. As can be seen, Sorbent calcining at 700℃ for 1 h produced $CaCO_3$ at 2θ of 29.7° and 47.8°. This shows that the decomposition of

$CaCO_3$ to CaO on calcination of stone sludge powder at 700℃ for 1 h still was not completed, and calcined samples contained $CaCO_3$ as the major phase and CaO as a minor one. In addition, the $CaFe_2O_4$ peaks were rarely identified.

EDX is a semi-quantitative technique for chemical analysis of samples in SEM method. The chemical composition of samples could be derived via subsequent analysis of gained peaks as well as comparison with reference peak data (Sarjeant, 2014). Here, EDX analysis shows the presence of calcium and oxygen with concentrations of 48 wt.% and 44 wt.%, respectively, along with low concentration of iron (5.4 wt.%) and silicon (2.3 wt.%) in the uncalcined sample. Fig. 4 presents the peaks of EDX analysis.

Results show a decrease in the oxygen content of the sample, which was due not only to the decomposition of $CaCO_3$ but to the release of CO_2. Based on this analysis, the large composition of the calcined sample was calcium and oxygen with concentrations of 51 wt.% and 42 wt.%, respectively, followed by iron and silicon with concentrations of 5 wt.% and 3 wt.%, respectively.

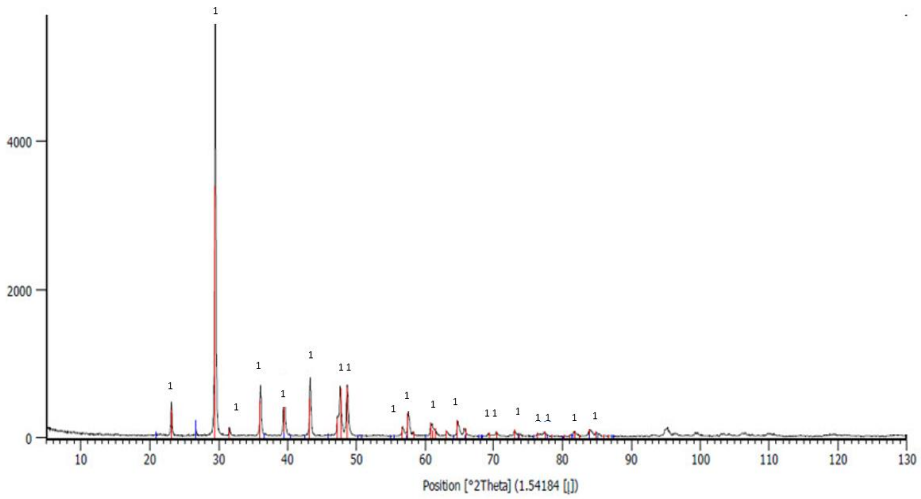

Fig. 2. X-ray diffraction analysis of uncalcined stone sludge powder in position [2Θ] (Note: 1=$CaCO_3$)

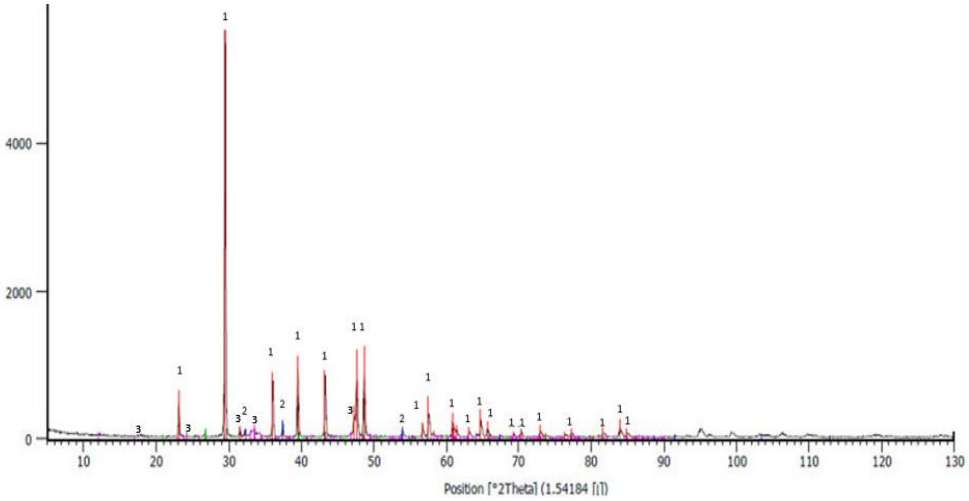

Fig. 3. X-ray diffraction analysis of calcined stone sludge powder at 700 C° in position [2Θ] (Note: 1=$CaCO_3$, 2= CaO, 3= $CaFe_2O_4$)

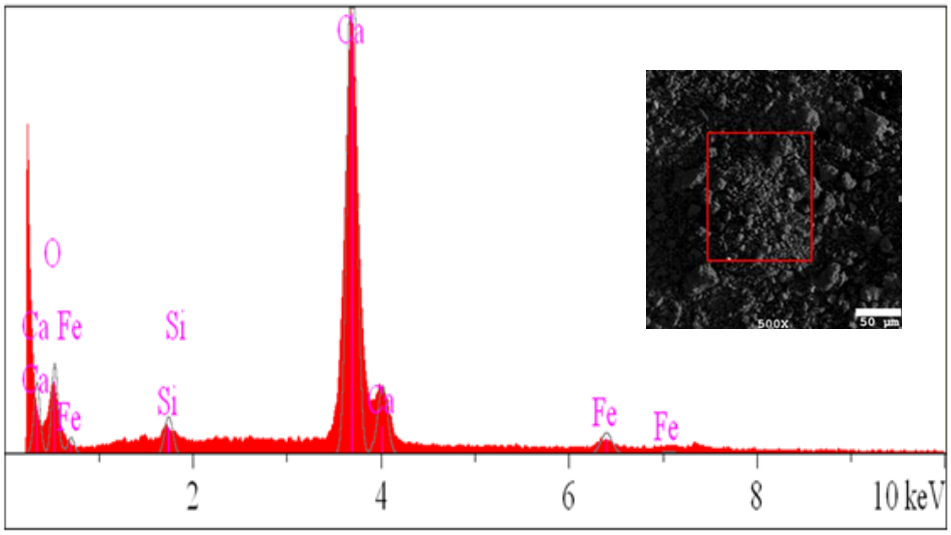

Fig. 4. EDX analysis of uncalcined stone sludge powder

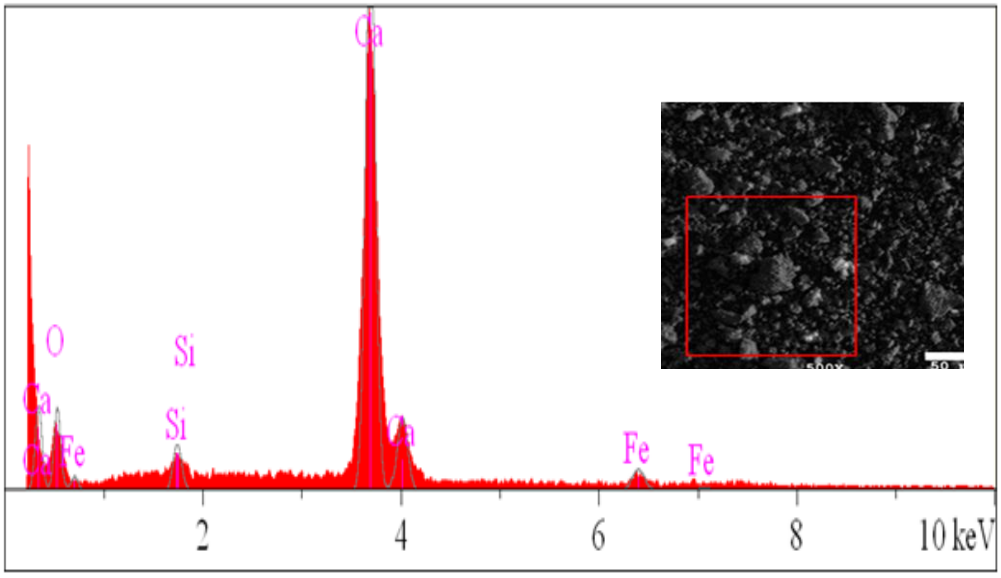

Fig. 5. EDX analysis of calcined stone sludge powder at 700 C°

Like uncalcined sorbent, the EDX analysis was done to determine the changes, occurring during calcination at 700℃. Based on its results, the decrease of oxygen content of the sample was due to both decomposition of $CaCO_3$ and partial release of oxygen and carbon in the CO_2. According to this analysis, the major elements of the calcined sample were calcium and oxygen with concentrations of 50.17 wt.% and 41.84 wt.%, followed by iron and silicon with concentrations of 5.3 wt.% and 2.77 wt.%, respectively. Fig. 5 gives EDX peaks of calcined stone sludge powder.

Fig. 3a illustrates the SEM image of uncalcined stone sludge powder in magnifications of X15, showing the morphological structure of adsorbent particles. The images obviously prove that the particles of adsorbent joined one another, resulting in an agglomerated structure. According to Fig. 6, some of the particles were more compact and many small granular particles were attached to their surface. In

addition, the surface seemed to be smooth and the structure, dense; thus, the porosity was low. The image also shows that the particle size in uncalcined samples was about 75 nm.

Fig. 7 (X15) demonstrates the SEM image of calcined stone sludge powder at 700℃, representing the same condition with uncalcined samples in terms of particle agglomeration. As can be seen in Fig. 3b, the surface of the calcined sample was rough and porous and small isolated particles also found. The measurements also indicated that the size of calcined stone sludge powder was approximately 100 nm.

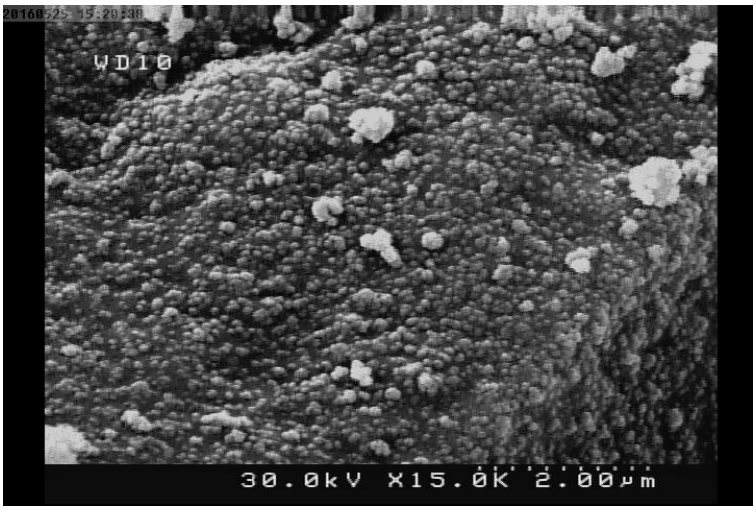

Fig. 6. SEM images of raw stone sludge X15

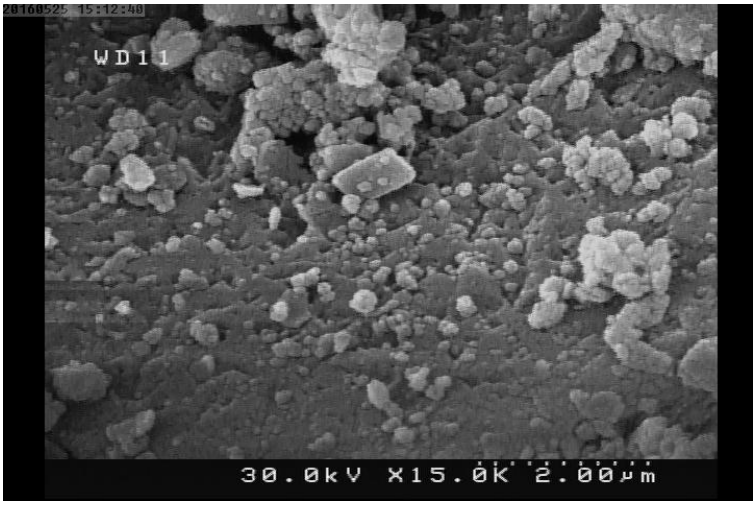

Fig. 7. SEM images of X15 stone sludge powder, calcined at 700 °C

Table 1 represents the value of BET parameters for uncalcined and calcinated adsorbents. As can be seen, the surface area increased partially during incomplete calcination process, which is considered the most important factors in the adsorption process. The mean pore diameter of both adsorbents were more than 2 nm and less than 50 nm; hence, it can be concluded that the stone sludge powder particles were mesoporous (Atwood & Steed, 2004). Like surface area, as a result of incomplete calcination, the total pore volume ($P/P_{0)}$ was enhanced slightly.

Figs. 8 and 9 show the diagrams of pore size distribution of uncalcined and calcined stone sludge powders, obtained via BJH method. According to these figures, the

stone sludge powder particles in both sample types had a multimodal pore size distribution with pores smaller than 10 nm.

Figs. 10 and 11 illustrate nitrogen adsorption and desorption isotherms of the adsorbents, respectively. Based on IUPAC, the nitrogen adsorption and desorption isotherm are classified into six types. In type I, the isotherms increase quickly at low relative pressures (P/P_0), thence to slow down at middle pressure. This type of isotherm indicates that adsorbent pores are micropore and mesopore. Type II adsorption isotherm is of an ascending type. By increasing the pressure, the monolayer adsorption turns to a multilayer mode, thanks to well-developed macropore. The absorbance further rises when the P/P0 value is close to 1. Type III adsorption isotherm displays a weak interaction between adsorbent and adsorbate. As for Type IV, the connectivity of pores with various sizes, on one hand, and the adsorbent, on the other, develops considerable micropore and mesopore, yet with the exception of non-macropore. The absorbance of Type V adsorption isotherm increases slowly, showing poorly developed micropores, only to soar significantly afterwards. Finally, Type VI isotherm is quite rare (Zhang et al., 2016).

Here, the isotherm pattern for uncalcined and calcined adsorbent corresponded to Type IV, according to IUPAC classification. This type of isotherm is characteristic of solids with mesopores. In Type IV isotherm, the slope rises at higher elevated pressures, indicating an increased uptake of adsorbate molecule as the pores are being filled (Aligizaki, 2014).

Table 2. Surface and pore characteristics of uncalcined and calcined stone sludge powder

Adsorbent	BJH plot			BET plot		
	V_p (cm^3/g)	S_p (m^2/g)	P/P_0 (cm^3/g)	V_m (cm^3/g)	d_p (nm)	S_a (m^2/g)
Calcined	0.00268	2.3	0.00291	0.64	4.19	2.78
Uncalcined	0.00731	5.3	0.00814	1.55	4.83	6.75

V_p primary mesopore volume; S_p specific surface area of primary mesopores; P/P_0 total pore volume; V_m monolayer volume; d_p mean pore diameter; and S_a BET specific surface area

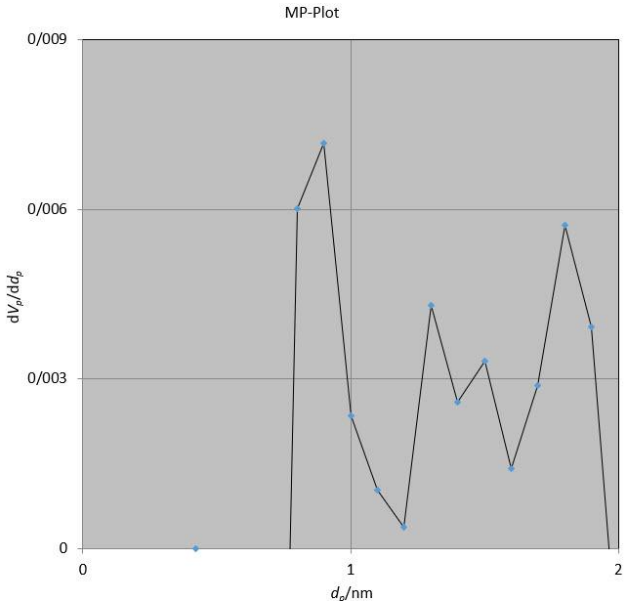

Fig. 8. Pore size distribution of uncalcined stone sludge

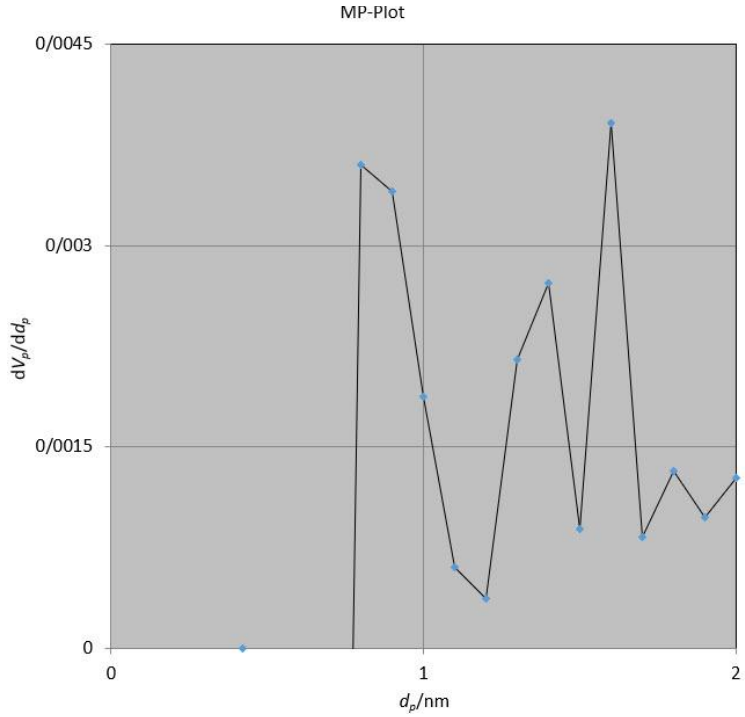

Fig. 9. Pore size distribution of calcined stone sludge

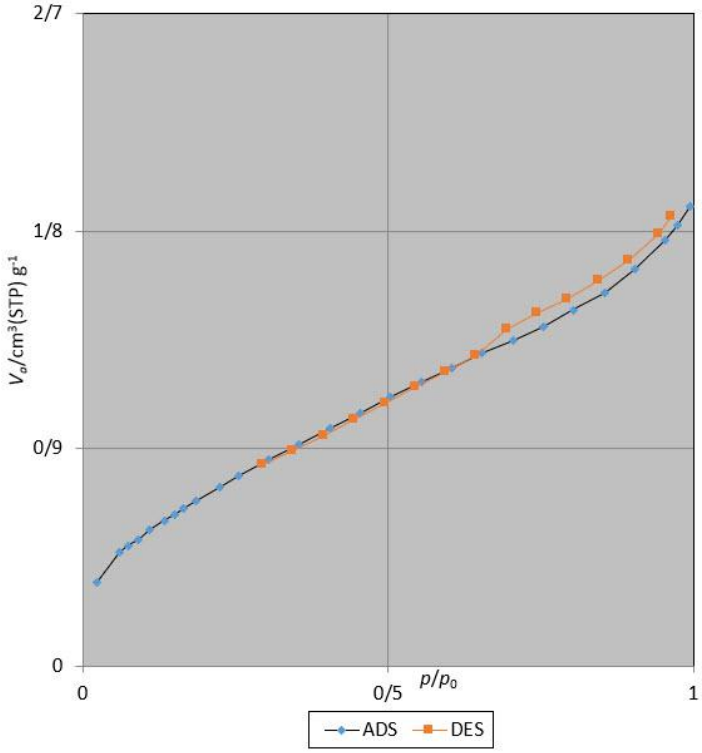

Fig. 10. Nitrogen adsorption and desorption isotherm for uncalcined stone sludge

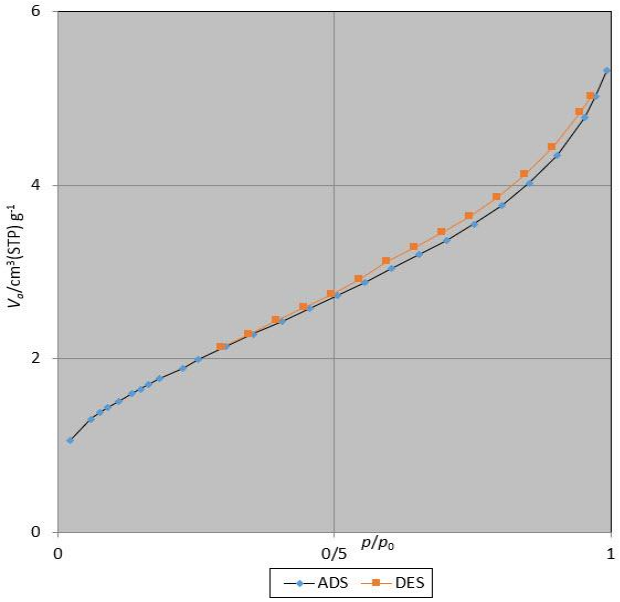

Fig. 11. Nitrogen adsorption and desorption isotherm for calcined stone sludge

Desulfurization tests were conducted with various amounts of stone sludge powder, including 0.1, 0.3, 0.5, 0.7, and 1 g. Fig. 12 represents the average percentage of SO_2 adsorption for each adsorbent amount per time unit. The SO_2 removal percentages were 5.1%, 8%, 10.3%, 18.13%, and 32.3% for 0.1, 0.3, 0.5, 0.7, and 1 g of adsorbent, respectively. As can be seen, SO_2 removal got boosted via increasing the amount of the adsorbent. In general, vacant adsorption sites and the surface area increase with an increase in the adsorbent dosage, consequently leading to a rise in adsorption capacity (Gökçekus et al., 2011; Lichtfouse et al., 2011; Regupathi et al., 2016). The higher availability of exchangeable sites leads to enhancement of adsorbed molecules (Lewinsky, 2007). Sirisha et al. (2012) studied SO_2 adsorption, using alum sludge (Sirisha et al., 2012). They observed that by raising the alum dosage from 0.2 g to 1 g, the removal percentage of SO_2 increased. Priyanka et al. (2012) used *Macrotyloma uniflorum* seed powder as an adsorbent of SO_2 (Priyanka et al., 2012). By increasing the seed powder's amount from 0.2 to 0.4 g, SO_2 removal percentage rose by %10 approximately.

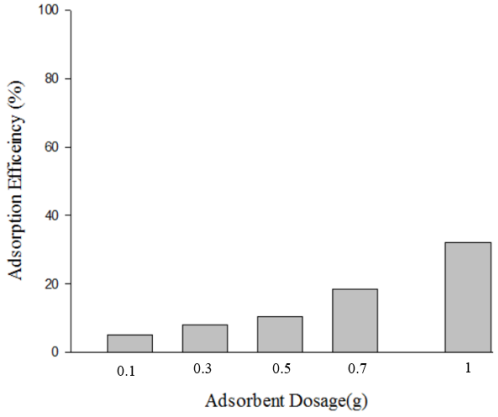

Fig. 12. The average percentage of SO_2 adsorption for various amounts of stone sludge (SO_2 concentration: 588 ppm, SO_2 volume: 1.3 Lit, test duration: 25min, and flow rate: 50 ml/min)

The stone sludge powder was calcined at 400, 500, 600, and 700℃ for 1 h. Results (Fig. 13) show that by increasing the calcination temperature from 400 to 700℃, the adsorbent efficiency ascended from 36.6% for the raw sample to 63.8% for the calcined one at 700℃. Since the surface area and the porosity was raised in the thermal treatment, the calcined samples were capable of adsorbing more SO_2. Agnew et al. (2005) reported low surface area of limestone and formation of a non-permeable product sulfide layer around the outside of the particle (Agnew et al., 2005), which resulted in poor conversion to sulfide. When limestone reacts at non-calcining conditions, conversion is restricted to approximately surface coverage. Fenouil and Lynn (1995) and Valek et al. (2014) observed the higher reactivity of CaO as the sorbent in comparison with the raw limestone (Fenouil & Lynn, 1995; Válek et al., 2014). Large surface areas and well-developed pore structures allow a prolonged sulfidation reaction. Borgwardt (1989) found that a large surface area, presented for the reaction, allowed much higher conversions when CaO reacted to SO_2 (Borgwardt, 1989).

Another explanation is related to the role of compounds like Fe_2O_3, MgO, Al_2O_3, ZnO, and Si_2O, which might be in a separate phase with CaO grains (Souza et al., 2010). Among these compounds, one of the most promising oxides is iron oxide, thanks to its high capacity and reactivity, good regenerability, and cost-effectivene nature (Fan et al., 2007). Yang et al. (2008) studied the kinetic behavior of Fe_2O_3 in desulfurization, reporting that Fe_2O_3 along with CaO and ZnO_2 had a considerable capacity for adsorption of SO_2 per gram of sorbent (Yang et al., 2008). Davini (2000) and Siagi et al. (2007) pointed out that iron oxide plays a very important role in desulfurization even in small amounts, probably in relation to the catalytic role of iron in the oxidation process of SO_2 to SO_3 as well as reaction with solid CaO particles (Davini, 2000; Siagi et al., 2007).

Another noteworthy result of this study was the observation of $CaFe_2O_4$ peaks, happening by means of XRD analysis of the calcined sample. The compound is a product of the reaction of CaO and Iron (III) Oxide. In this regard, CaO can stabilize Fe^{3+} by forming $CaFe_2O_4$ ($CaO.Fe_2O_3$), thus making it more effective (Fan et al., 2007).

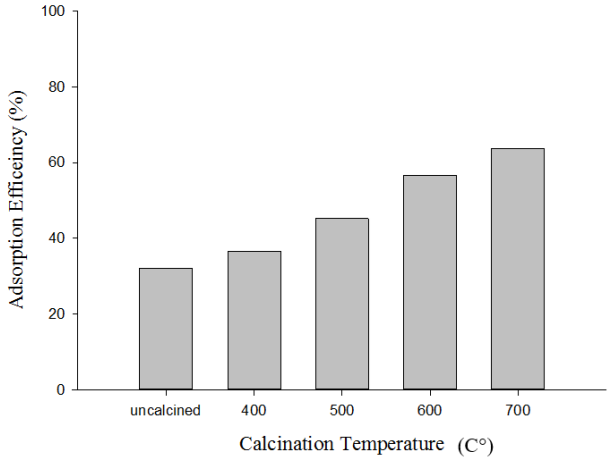

Fig. 13. Average percentage of SO_2 adsorption by calcined stone sludge at different temperatures (SO_2 concentration: 588 ppm, SO_2 volume: 1.3 L, test duration: 25min, flow rate: 50 ml/min, adsorbent dose: 1g, and reaction temperature: 25C°).

The experiments were performed with 1 g of the adsorbent, having varied humidity contents like 1%, 5%, and 10 wt.%. Results indicate that the adsorption efficiency of raw stone sludge got enhanced with an increase in the adsorbent humidity content from 0 to 10% (Fig. 14). The maximum adsorption percentage was 76.3% for the adsorbent with 10 wt.% humidity. The average percentages of sulfur dioxide adsorption by calcined stone sludge powder at 700℃ with 0%, 1%, 5%, and 10% humidity contents equaled to 63.8%, 71.6%, 83.4%, and 94.1%, respectively (Fig. 15). The humidified adsorbents from hydration of SO_2 by adsorbed water molecules on the adsorbent surface were more effective for desulfurization. Siagi et al. (2006) reported that the relative humidity is a major factor in the ability of dolomite and limestone to capture SO_2 (Siagi et al., 2006). Liu et al. (2002) used the mixture of $Ca(OH)_2$ with fly ash as an adsorbent of SO_2, showing that by increasing the relative humidity, the reaction rate boosted significantly (Liu et al., 2002).

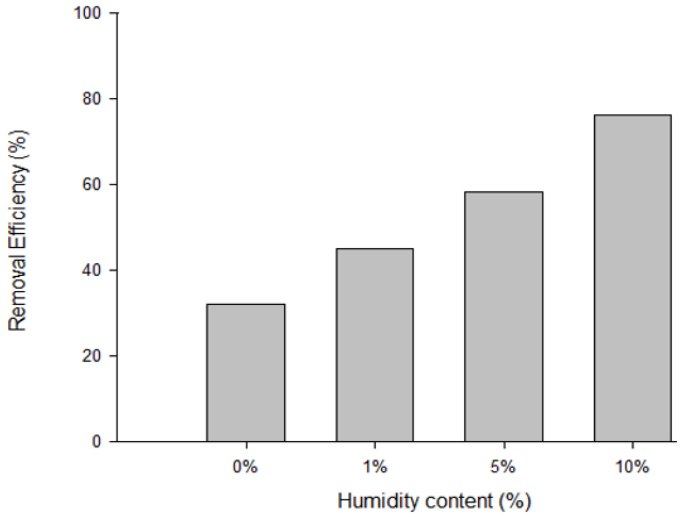

Fig. 14. Average percentage of SO_2 adsorption by uncalcined stone sludge with different humidity contents (SO_2 concentration: 588 ppm, SO_2 volume: 1.3 L, test duration: 25min, and flow rate: 50 ml/min)

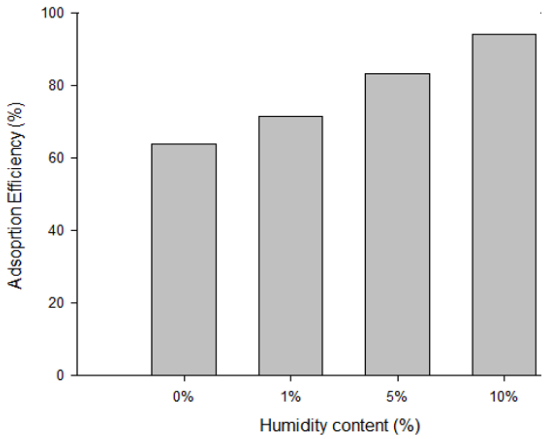

Fig. 15. Average percentage of SO_2 adsorption by calcined stone sludge at 700 C° with different humidity contents (SO_2 concentration: 588 ppm, SO_2 volume: 1.3 L, test duration: 25min, flow rate: 50 ml/min, adsorbent dose: 1g, and reaction temperature: 25°C).

CONCLUSION

Stone sludge powder was used to remove sulfur dioxide. The effect of the adsorbent amount, thermal modification, and humidity content of adsorbent on the adsorption efficiency was studied. Results revealed that an increase in the adsorbent dose raised adsorption efficiency. Humidity content had a great effect on SO_2 removal by uncalcined and calcined adsorbents. By raising humidity content up to 10 wt.%, the adsorption efficiency increased remarkably. Generally, the results indicated that the calcareous stone sludge was well potential to be used in adsorption of sulfur dioxide, particularly because of their low cost. This could be suggested as a method for waste management in stone industries.

REFERENCES

Yang, H. Xu, Z. Fan, M. Gupta, R. Slimane, R.B. Bland, A.E. and Wright, I. (2008). Progress in carbon dioxide separation and capture: A review. J. Environ. Sci., 20(1); 14-27.

Chakrabarti, P.D. (2001). Urban crisis in India: New initiatives for sustainable cities. Devel. Prac., 11(2-3); 260-272.

Nath, B. and Stefanov Cholakov, G. (2009). Pollution control technologies EOLSS Publications. The United Kingdom; 124-153.

Córdoba, P. (2015). Status of flue gas desulfurization (FGD) systems from coal-fired power plants: Overview of the physic-chemical control processes of wet limestone FGDs. Fuel., 144(274-286.

Rayaprolu, K. (2017). Boilers: A practical reference (1 ed). CRC Press 159-160.

Suárez-Ruiz, I. and Crelling, J.C. (2008). Applied coal petrology: The role of petrology in coal utilization Academic Press. 111-127.

Miao, M. Feng, X. Wang, G. Cao, S. Shi, W. and Shi, L. (2015). Direct transformation of FGD gypsum to calcium sulfate hemihydrate whiskers: Preparation, simulations, and process analysis. Particulogy., 19(53-59.

Xie, W. Chang, L. Wang, D. Xie, K. Wall, T. and Yu, J. (2010). Removal of sulfur at high temperatures using iron-based sorbents supported on fine coal ash. Fuel., 89(4); 868-873.

Lees, D. and Payne, J. (2001). Chemistry for ocr a for separate award Pearson Education. 22-32.

Gopi, S. (2009). Basic civil engineering Pearson Education India. 9-11.

Lorpari Zanganeh, A. and Roosta, A. (2012). Analytical study of Iran export and manufacturing of decorative stones in the year 2012 (2012 – 2013) and Iran's position in the global decorative stone industry. Int. J. Sc. Manag. Devel. 3(1); 793-798. ISSN:2345-3974.

Lakhani, R. Kumar, R. and Tomar, P. (2014). Utilization of stone waste in the development of value-added products: A state of the art review. J. Eng. Sci. Tech. Rev., 7(3); 180-187.

Almeida, N. Branco, F. and Santos, J.R. (2007). Recycling of stone slurry in industrial activities: Application to concrete mixtures. J. Build. Env., 42(2);810-819.

Al-Joulani, N. (2007). Engineering properties, industrial and structural applications of stone slurry waste. J. J. App. Sci., 9(1); 13-23.

Al-Joulani, N. (2014). Utilization of stone slurry powder in the production of artificial stones. Re. J. Eng. App. Sci., 3(4); 245-249.

Alzboon, K. K. and Mahasneh, K. N. (2009). Effect of using stone cutting waste on the compression strength and slump characteristics of concrete. Int. J. Env. Sci. Eng, 1(4); 167-172.

Barani, K. and Esmaili, H. (2016). Production of artificial stone slabs using waste granite and marble stone sludge samples. J. Min. Env., 7(1); 135-141.

Pappu, A. Saxena, M. and Asolekar, S.R. (2007). Solid wastes generation in India and their recycling potential in building materials. Build. Environ., 42(6); 2311-2320.

Altun, N. E. (2014). Assessment of marble waste utilization as an alternative sorbent to limestone for SO2 control. Fuel Process. Technol., 128(461-470).

Maina, P. and Mbarawa, M. (2012). Blending lime and iron waste to improve sorbents reactivity towards desulfurization. Fuel., 102(162-172).

Ogenga, D. Mbarawa, M. Lee, K. Mohamed, A. and Dahlan, I. (2010). Sulfur dioxide removal using south African limestone/siliceous materials. Fuel., 89(9); 2549-2555.

Siagi, Z. Mbarawa, M. Mohamed, A. Lee, K. and Dahlan, I. (2007). The effects of limestone type on the sulfur capture of slaked lime. Fuel., 86(17-18); 2660-2666.

Saravanan, R. and Rani, M.P. (2011). Metal and alloy bonding-an experimental analysis: Charge density in metals and alloys. Springer Science & Business Media. 32-40.

Sahoo, S. Chakraborti, C. K. Mishra, S. C. and Nanda, U. N. (2011). Scanning electron microscopy as an analytical tool for particle size distribution and aspect ratio analysis of ciprofloxacin mucoadhesive polymeric suspension. Academic Research Publishing Agency., 6(6); 1-11.

Gladysz, G. M. and Chawla, K. K. (2014). Voids in materials: From unavoidable defects to designed cellular materials. Elsevier., 169-170.

Lin, R. B. Shih, S. M. and Liu, C. F. (2003). Characteristics and reactivities of ca (oh) 2/silica fume sorbents for low-temperature flue gas desulfurization. Chem. Eng. Sci., 58(16); 3659-3668.

Stanmore, B. and Gilot, P. (2005). Calcination and carbonation of limestone during thermal cycling for CO2 sequestration. Fuel Process. Technol., 86(16); 1707-1743.

Ismail, H. Shamsudin, R. Hamid, M. A. A. and Awang, R. (2016). Characteristics of β-wollastonite derived from rice straw ash and limestone. J. Aust. Ceram. Soc., 52(2); 163-174.

Souza, F. D. and Braganca, S. R. (2017). Evaluation of limestone impurities in the desulfurization process of coal combustion gas. Braz. J. Chem. Eng., 34(1); 263-272.

Sarjeant, C. (2014). Contextualizing the Neolithic occupation of southern Vietnam (terra australis 42) ANU Press. Canberra, 482 p.

Atwood, J.L. and Steed, J.W. (2004). Encyclopedia of supramolecular chemistry CRC Press. 950-995.

Zhang, Y. Shao, D. Yan, J. Jia, X. Li, Y. Yu, P. and Zhang, T. (2016). The pore size distribution and its relationship with shale gas capacity in organic-rich mudstone of Wufeng-Longmaxi formations, Sichuan basin, China. J. Natu. Gas. Geosci., 1(3); 213-220.

Aligizaki, K. K. (2014). Pore structure of cement-based materials: Testing, interpretation, and requirements CRC Press. 60-108.

Gökçekus, H. Türker, U. and LaMoreaux, J. W. (2011). Survival and sustainability: Environmental concerns in the 21st century Springer Science & Business Media. 903-904.

Lichtfouse, E. Schwarzbauer, J. and Robert, D. (2011). Environmental chemistry for a sustainable world: Volume 2: Remediation of air and water pollution Springer Science & Business Media.

Regupathi, I. Shetty, V. and Thanabalan, M. (2016). Recent advances in chemical engineering Springer. 158-162.

Lewinsky, A.A. (2007). Hazardous materials and wastewater: Treatment, removal and analysis Nova Publishers. 201-224.

Sirisha, D. Mukkanti, K. and Gandhi, N. (2012). Adsorption studies on alum sludge. Adv. Appl. Sci. Re, 3(5); 3362-3366.

Priyanka, V. M. Sirisha, D. and Gandhi, N. (2012). Sulfur dioxide adsorption using macrotyloma uniflorum lam. Seed powder. Proceedings of the International Academy of Ecology and Environmental Sciences., 2(4); 251-254.

Agnew, J. Hampartsoumian, E. Jones, J. and Nimmo, W. (2005). The effect of sintering on sulfur capture by limestone and dolomite. J. Energy. Inst., 78(2); 81-89.

Fenouil, L. A. and Lynn, S. (1995). Study of calcium-based sorbents for high-temperature h2s removal. 1. Kinetics of h2s sorption by uncalcined limestone. Ind. Eng. Chem. Res., 34(7); 2324-2333.

Válek, J. Van Halem, E. Viani, A. Pérez-Estébanez, M. Ševčík, R. and Šašek, P. (2014). Determination of optimal burning temperature ranges for production of natural hydraulic limes. Constr. Build. Mater., 66; 771-780.

Borgwardt, R. H. (1989). Calcium oxide sintering in atmospheres containing water and carbon dioxide. Ind. Eng. Chem. Res., 28(4); 493-500.

Souza, A. Pinheiro, B. and Holanda, J. (2010). Recycling of gneiss rock waste in the manufacture of vitrified floor tiles. J. Environ. Manage., 91(3); 685-689.

Fan, H. Xie, K. Shangguan, J. Shen, F. and Li, C. (2007). Effect of calcium oxide additive on the performance of iron oxide sorbent for high-temperature coal gas desulfurization. J. Nat. Gas. Chem., 16(4); 404-408.

Davini, P. (2000). The investigation into the desulphurization properties of by-products of the manufacture of white marbles of northern tuscany. Fuel., 79(11); 1363-1369.

Siagi, Z. Mbarawa, M. Mohamed, A. Lee, K. and Dahlan, I., 2006. Removal of sulfur dioxide by calcium-based materials from different sources in south Africa, the 8th Asia-Pacific international symposium on combustion and energy utilization, Sochi (Russian Federation), pp. 10-12.

Liu, C. F. Shih, S. M. and Lin, R. B. (2002). Kinetics of the reaction of ca (oh) 2/fly ash sorbent with SO2 at low temperatures. Chem. Eng. Sci., 57(1); 93-104.